Journal of Experimental Botany, Vol. 66, No. 20 pp. 6327–6343, 2015
doi:10.1093/jxb/erv344 Advance Access publication 9 July 2015

RESEARCH PAPER

A subgroup of *MATE* transporter genes regulates hypocotyl cell elongation in *Arabidopsis*

Rui Wang*, Xiayan Liu*, Shuang Liang, Qing Ge, Yuanfeng Li, Jingxia Shao, Yafei Qi, Lijun An and Fei Yu†

State Key Laboratory of Crop Stress Biology in Arid Areas and College of Life Sciences, Northwest A&F University, Yangling, Shaanxi 712100, China

* These authors contributed equally to this work.
† To whom correspondence should be addressed. E-mail: flyfeiyu@gmail.com

Received 9 April 2015; Revised 4 June 2015; Accepted 15 June 2015

Editor: James Murray

Abstract

The growth of higher plants is under complex regulation to ensure the elaboration of developmental programmes under a changing environment. To dissect these regulatory circuits, we carried out genetic screens for *Arabidopsis abnormal shoot* (*abs*) mutants with altered shoot development. Here, we report the isolation of two dominant mutants, *abs3-1D* and *abs4-1D*, through activation tagging. Both mutants showed a 'bushy' loss of apical dominance phenotype. *ABS3* and *ABS4* code for two closely related putative Multidrug and Toxic Compound Extrusion (MATE) family of efflux transporters, respectively. *ABS3* and *ABS4*, as well as two related *MATE* genes, *ABS3-Like1* (*ABS3L1*) and *ABS3L2*, showed diverse tissue expression profiles but their gene products all localized to the late endosome/prevacuole (LE/PVC) compartment. The over-expression of these four genes individually led to the inhibition of hypocotyl cell elongation in the light. On the other hand, the quadruple knockout mutant (*mateq*) showed the opposite phenotype of an enhanced hypocotyl cell elongation in the light. Hypocotyl cell elongation and de-etiolation processes in the dark were also affected by the mutations of these genes. Exogenously applied sucrose attenuated the inhibition of hypocotyl elongation caused by *abs3-1D* and *abs4-1D* in the dark, and enhanced the hypocotyl elongation of *mateq* under prolonged dark treatment. We determined that *ABS3* genetically interacts with the photoreceptor gene *PHYTOCHROME B* (*PHYB*). Our results demonstrate that ABS3 and related MATE family transporters are potential negative regulators of hypocotyl cell elongation and support a functional link between the endomembrane system, particularly the LE/PVC, and the regulation of plant cell elongation.

Key words: *Abnormal shoot* mutant, cell elongation, de-etiolation, endosome, MATE transporter, photomorphogenesis.

Introduction

Higher plant development in the light follows a well-characterized programme known as photomorphogenesis (Chen *et al.*, 2004). In contrast, when grown in the dark, higher plants follow a different developmental pathway termed skotomorphogenesis (Chory *et al.*, 1989). For both photo- and skotomorphogenesis, complex genetic regulatory networks govern the elaboration of these developmental programmes (Jiao *et al.*, 2007; Lau and Deng, 2010; Arsovski *et al.*, 2012). One hallmark distinction between plants grown in the light and in the dark is the differential regulation of hypocotyl

Abbreviations: *abs, abnormal shoot* mutant; ER, endoplasmic reticulum; LE/PVC, late endosome/prevacuole; MATE, Multidrug and Toxic Compound Extrusion; MDR, multidrug resistance; *TT12, TRANSPARENT TESTA12*; WT, wild type.

© The Author 2015. Published by Oxford University Press on behalf of the Society for Experimental Biology. All rights reserved.
For permissions, please email: journals.permissions@oup.com

Downloaded from https://academic.oup.com/jxb/article/66/20/6327/552696 by guest on 24 April 2024

cell elongation with short hypocotyls in the light and elongated hypocotyls in the dark, and this simple yet powerful system has facilitated great progresses in plant developmental genetics. For example, *long hypocotyl* (*hy*) mutants have been instrumental in the establishment of our current understanding of light perception and light's inhibitory effect on hypocotyl cell elongation (Arsovski *et al.*, 2012). On the other hand, *de-etiolated* (*det*)/*constitutive photomorphogenesis* (*cop*)/*fusca* (*fus*) mutants display light-grown characteristics in the dark, particularly the shortened hypocotyls (Chory *et al.*, 1989; Deng *et al.*, 1991; Castle and Meinke, 1994; Miséra *et al.*, 1994).

Among the myriads of genes that are involved in the regulation of plant development, an emerging group is the multidrug resistance (MDR) transporter genes. The roles of MDR proteins in biology have been more prominently implicated in the efflux of antibiotics from pathogenic bacteria and thus multidrug resistance in humans and other organisms (Monk and Goffeau, 2008; Nikaido, 2009). Not surprisingly, MDRs are also vital regulatory components in plants. For example, MDR-like proteins AtMDR1 and AtPGP1 are required for phytohormone auxin-mediated plant development (Noh *et al.*, 2001, 2003). Under the broad definition of multidrug efflux transporters are five major families: the major facilitator superfamily (MFS); the resistance-nodulation-division (RND) superfamily; the ATP-binding cassette (ABC) superfamily; the small multidrug resistance (SMR) superfamily and the multidrug and toxic compound extrusion (MATE) superfamily (Nikaido, 2009). Among these families, the founding member of MATE family of transporters NorM was reported in *Vibrio parahaemolyticus* (Morita *et al.*, 1998). When expressed in *Escherichia coli*, NorM can carry out the efflux of antibiotics including norfloxacin and confer resistance to norfloxacin and a host of antibiotics (Morita *et al.*, 2000).

In the model plant *Arabidopsis thaliana*, there are at least 56 *MATE* family transporter genes (Li *et al.*, 2002). A number of *Arabidopsis MATE* genes have been characterized and have been implicated in a diverse array of developmental and metabolic processes. The most well characterized *Arabidopsis MATE* gene is the *TRANSPARENT TESTA12* (*TT12*) (Debeaujon *et al.*, 2001). *TT12* gene was first identified in a genetic screen for *Arabidopsis* mutants with altered seed testa colour (Debeaujon *et al.*, 2001). Loss of *TT12* confers a paler brown seed colour when compared with wild-type seeds and *TT12* is expressed at seed coat endothelium, suggesting a role for TT12 in the deposition of flavonoids that are responsible for the brown WT seed colour. Further studies showed that TT12 is located at the tonoplast and functions as a vacuolar flavonoid/H^+ antiporter involved in the synthesis of proanthocyanidin in *Arabidopsis* and *Medicago trunculata* (Marinova *et al.*, 2007; Zhao and Dixon, 2009).

Other members of the *Arabidopsis* MATE transporter family have been implicated in toxin sensitivity (Diener *et al.*, 2001), pathogen responses (Nawrath *et al.*, 2002; Sun *et al.*, 2011), heavy metal detoxification (Li *et al.*, 2002), iron responses (Rogers and Guerinot, 2002; Seo *et al.*, 2012) and organogenesis (Burko *et al.*, 2011; Li *et al.*, 2014). In sorghum, a *MATE* family gene has been linked with aluminum tolerance (Magalhaes *et al.*, 2007). Although a growing list of MATE transporters are being characterized, the functions of the majority of MATE family members remain poorly understood.

We are interested in the genetic regulation of plant development and have initiated screens in *Arabidopsis* to look for mutants with altered developmental programmes. In an activation tagging mutant population, we identified two mutants we named *abnormal shoot3-1D* (*abs3-1D*) and *abs4-1D*. These two semi-dominant mutants show almost identical phenotypes of increased leaf initiation, early flowering and loss of apical dominance. The cloning of *ABS3* revealed that it encodes a putative MATE family transporter. Interestingly, *ABS4* encodes a second putative MATE family transporter. In addition, we found that ectopic over-expression of two *ABS3* homologous genes, *ABS3-Like1* (*ABS3L1*) and *ABS3L2*, caused similar phenotypes. We determined that *ABS3*, *ABS4*, *ABS3L1* and *ABS3L2* have distinct expression patterns but their gene products all likely localize to the late endosome/prevacuole (LE/PVC) compartment. Further characterizations revealed that the over-expression of these four *MATE* genes leads to reduced hypocotyl cell elongation, while quadruple loss-of-function mutants showed the opposite effect of promoting hypocotyl cell elongation in the light. Moreover, *ABS3* or *ABS4* over-expression leads to reduced hypocotyl cell elongation in the dark, i.e. a de-etiolation/constitutive photomorphogenesis phenotype in the dark, similar to the well-known *det*/*cop*/*fus* mutants. Suppressor work indicated that *ABS3* genetically interacts with the photoreceptor gene *phytochrome B*. Our findings reveal previously unknown capacities of the *MATE* family of transporter genes as regulators of plant cell elongation both in the light and in the dark.

Materials and methods

Plant materials and growth conditions

All *Arabidopsis* strains used in this study are in the Columbia ecotype background except *phyB-1*, which is in the Landsberg *erecta* background (Reed *et al.*, 1993). *abs3-1D* was recovered in an activation tagging screen in *var2-5* mutant background (Yu *et al.*, 2008) and backcrossed with wild type (WT) to remove the *var2-5* mutation. All further characterizations of *abs3-1D* were carried out in the WT background. *abs4-1D* was recovered in an independent activation tagging screen in the WT background. The endoplasmic reticulum (ER) marker line (ER-gk CS16251) and the tonoplast marker line (vac-gk CS16257) were described by Nelson *et al.* (2007). The Golgi marker line (WAVE22Y) was described by Geldner *et al.* (2009). Organelle marker lines and T-DNA insertion lines SM3_36823 (*abs3-1*), SALK_067667 (*abs4-1*), SAIL_1236_H10 (*abs3l1-1*) and SALK_144096 (*abs3l2-1*) were obtained from the Arabidopsis Resource Center (ABRC). All T-DNA lines were confirmed by PCR and sequencing and backcrossed with WT to clear background mutations prior to further analysis. Primers used to genotype T-DNA mutants are listed in Supplementary Table S1.

All plants were maintained under continuous illumination at 22°C unless otherwise specified. Fluorescence bulbs (TL-D 36W/865, Philips) were used as the light source to grow *Arabidopsis*. The light intensity was ~100 μmol m^{-2} s^{-1}.

Downloaded from https://academic.oup.com/jxb/article/66/20/6327/552696 by guest on 24 April 2024

DNA and RNA manipulations

Total genomic DNA extraction, plasmid rescue, southern blot and northern blot analyses were performed as described (Yu *et al.*, 2008). Total RNA purification and semi-quantitative RT-PCR analysis were performed as described (Wang *et al.*, 2012). All primers used in this study are listed in Supplementary Table S1.

Generation of ABS3, ABS4, AB3L1 *and* ABS3L2 *over-expressing lines*

Genomic or cDNA fragments encompassing the open reading frames (ORFs) of *ABS3*, *ABS4*, and *ABS3L1*, *ABS3L2* were amplified by primers 29140F and 29140R, 58340F and 58340R, 19700F and 19700R, and 52050F and 52050R, respectively. The amplified fragments were ligated into pBlueScript KS+ (pBS) and sequenced before subcloned into a binary vector pBI111L (Yu *et al.*, 2004). The resulting constructs were designated P_{35S}::*ABS3*, P_{35S}::*ABS4* and P_{35S}::*ABS3L1*, and P_{35S}::*ABS3L2*. *Arabidopsis* were transformed using the floral dip method (Clough and Bent, 1998). Transgenic lines were selected on half strength Murashige and Skoog (1/2 MS) medium (*Phyto*Technology Laboratories) supplemented with 1% (w/v) agar and 50 mg l^{-1} kanamycin.

Histochemical GUS assay

The promoter regions of *ABS3*, *ABS4*, *ABS3L1* and *ABS3L2* were amplified using primers 29140PF and 29140PR, 58340PF and 58340PR, 19700PF and 19700PR, and 52050PF and 52050PR, respectively. The amplified fragments were cloned into pBS, sequenced and subcloned into pCB308 (Xiang *et al.*, 1999). The resulting promoter-GUS constructs were introduced into WT. T1 plants were selected for Basta resistance. For each *MATE* gene promoter, histochemical GUS staining was performed on T2 plants from multiple independent lines at various growth stages (Jefferson, 1987).

Protoplast transient expression assay and subcellular localization analysis

Expression cassettes harbouring the 35S promoter and the coding sequences of GFP or mCherry fluorescent protein (with or without the stop codon) were first cloned into vectors of pBS or pUC18 backbone. The ORFs of *ABS3*, *ABS4*, *ABS3L1* and *ABS3L2* were subcloned into these vectors to have the fluorescent proteins fused to the N- or C-terminus of MATE proteins.

To check whether these MATE proteins share the same subcellular localization, P_{35S}::*ABS4-mCherry* was transiently co-expressed in WT leaf protoplasts with P_{35S}::*ABS3-GFP*, P_{35S}::*ABS3L1-GFP* or P_{35S}::*ABS3L2-GFP*, respectively. To establish the specific subcellular localization of ABS3 and its related MATE proteins, P_{35S}::*ABS3-GFP* or P_{35S}::*ABS4-mCherry* was transformed into protoplasts of stably transformed organelle marker lines or co-transformed with various organelle marker constructs generated in our lab into WT protoplasts. Detailed information of the organelle markers used in this study are listed in Supplementary Table S2. Leaf protoplast transient expression assays were performed as described in Yoo *et al.* (2007). An A1 con-focal microscope (Nikon) was used to monitor the signals of fluorescent fusion proteins.

Hypocotyl measurements

To measure the hypocotyl length, seeds were stratified in water at 4°C in the dark for 2 d before planting on 1/2 MS medium containing 1% (w/v) BACTO agar (BD). 1/2 MS medium supplemented with or without 1% (w/v) sucrose were used to assay hypocotyl elongation. For light-grown seedlings, plates were kept vertically at 22°C under continuous light (~100 μmol m^{-2} s^{-1}) for 7 d. For dark-grown seedlings, plates were placed under the light for 1 h to induce germination after stratification. Plates were then wrapped with aluminum foil and kept vertically in a light proof box at 22°C for 6 d or 20 d. Whole plates were photographed with a stereoscope equipped with a CCD camera (Nikon) and ImageJ software was used to measure the hypocotyl length. Statistical comparisons of the mean hypocotyl length of different genotypes were carried out using Student's *t*-test.

To visualize the outlines of hypocotyl epidermal cells, seedlings were stained with 1 mg ml^{-1} propidium iodide (PI) for 15 min and examined with an A1 confocal microscope (Nikon). Epidermal cells in the middle part of the hypocotyl were photographed.

Transmission electron microscopy

Cotyledons of 6-day-old dark grown WT and *ABS3* OE#5 seedlings were collected under dim-green safe light, and fixed in 0.1 M phosphate buffer (pH 7.2) containing 4% (v/v) glutaraldehyde overnight at 4°C. Samples were then post fixed in 1% osmium tetroxide in 0.1 M phosphate buffer, dehydrated and embedded in SPI-pon 812 resin (SPI Supplies). Ultrathin sections (80 nm) prepared with an EM UC7 ultramicrotome (Leica Microsystems) were stained with uranyl acetate and lead citrate, and examined by a Hitachi H-600 transmission electron microscope operated at 75 kV.

Results

Identification of two gain-of-function mutants, abs3-1D *and* abs4-1D

We previously carried out a large-scale activation tagging screen for genetic suppressors of the *var2* leaf variegation mutant (Yu *et al.*, 2008). In the same mutant population, we also systematically screened for mutants that displayed altered shoot development programmes and named them *abnormal shoot* (*abs*) mutants (Shao *et al.*, 2012; Wang, *et al.*, 2012). One mutant, designated *abs3-1D* (D for dominant), showed a semi-dominant loss-of-apical-dominance phenotype and was studied further (Fig. 1A–C). At juvenile stages, *abs3-1D* showed subtle yet reproducible phenotypes, including a more compact stature, likely the result of shortened petioles and an increased rate of leaf initiation (Fig. 1A). The phenotypes of *abs3-1D* were more conspicuous at reproductive stages. Compared to WT, *abs3-1D* bolted earlier and had an increased lateral branch development (Fig. 1B). Meanwhile, the elongation of the main inflorescence stem was inhibited in *abs3-1D*, giving rise to dwarf and bushy-appearing plants at mature stages (Fig. 1C). Siliques produced by *abs3-1D* were also reduced in length and contained fewer seeds (Fig. 1C). In a separate screen carried out in the WT background, we isolated another semi-dominant mutant *abs4-1D* that had highly similar, but slightly less severe phenotypes compared with those of *abs3-1D* (Fig. 1D–F).

We also generated double mutants of *abs3-1D* and *abs4-1D*. Compared with WT, *abs3-1D*, and *abs4-1D* double mutants were slightly more compact and showed more pronounced early flowering phenotype (Fig. 1G). The shoot branching phenotype was also more severe (Fig. 1G). Double mutants also showed further reduced fertility and were barely fertile (Fig. 1G). The interaction of *abs3-1D* and *abs4-1D* suggests that the ectopic effect of individual *abs3-1D* and *abs4-1D* mutants was not saturated and also the two mutants are likely to be disturbed in a similar way.

Downloaded from https://academic.oup.com/jxb/article/66/20/6327/552696 by guest on 24 April 2024

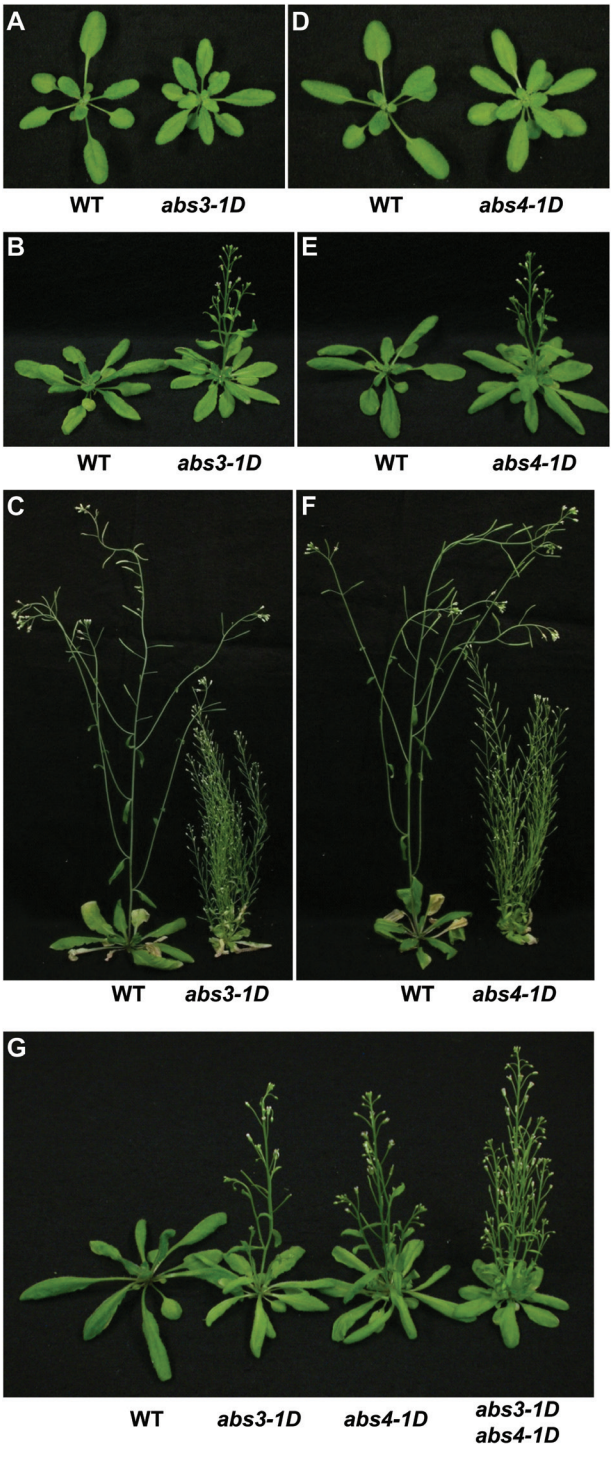

Fig. 1. Identification of *abs3-1D* and *abs4-1D* mutants. Overall plant architectures of *abs3-1D* (A–C) and *abs4-1D* (D–F) compared to that of WT of the same age. Plants were germinated and cultivated at 22°C under continuous light (~100 μmol m^{-2} s^{-1}). Illustrated are 3-week-old (A, D), 4-week-old (B, E) and 6-week-old plants (C, F). (G) Comparison of overall plant architectures of 4-week-old WT, *abs3-1D*, *abs4-1D* and *abs3-1D abs4-1D* double mutant.

Co-segregation analyses showed that both *abs3-1D* and *abs4-1D* were tightly linked with activation tagging T-DNAs and were likely caused by single T-DNA insertions (Supplementary Fig. S1). Plasmid rescues were carried out to determine the T-DNA insertion sites in *abs3-1D* and *abs4-1D*. Sequencing of the rescued plasmids revealed that for *abs3-1D* the T-DNA resided in the intergenic region on chromosome 4 between annotated genes At4g29130 and At4g29140, while the T-DNA was located on chromosome 1 between At1g58340 and At1g58350 in *abs4-1D* (Fig. 2A, B). Examination of the annotations of the genes adjacent to the T-DNA insertions revealed that At4g29140 and At1g58340 encode closely related putative MATE family transporters. Northern blots showed that the accumulations of At4g29140 and At1g58340 transcripts were greatly elevated in *abs3-1D* and *abs4-1D*, respectively (Fig. 2C, D). Considering the highly similar phenotypes of *abs3-1D* and *abs4-1D* and the semi-dominant nature of these mutants, it is likely that increased transcriptions of these two *MATE* transporter genes are the cause of mutant phenotypes.

To confirm that At4g29140 is *ABS3* and At1g58340 is *ABS4*, we generated independent transgenic lines over-expressing *ABS3* or *ABS4* in the WT background. In T1 and T2 generations, we isolated OE lines that had similar or more severe phenotypes compared with the original *abs3-1D* or *abs4-1D* mutant (Fig. 3A–D). The severity of the phenotype was in general correlated with the expression levels of *ABS3* or *ABS4* (Fig. 3A–D). At4g29140 was previously identified in activation tagging screens as *ADS1* (*ACTIVATED DISEASE SUSCEPTIBILITY1*; Sun *et al.*, 2011) and *ADP1*

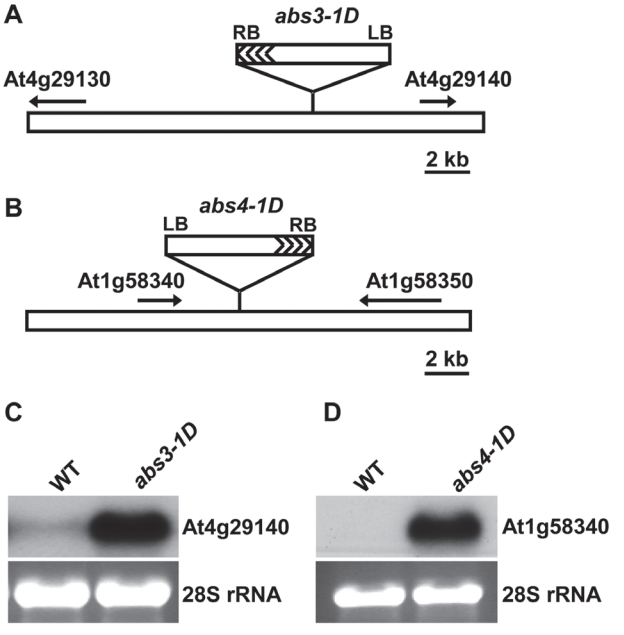

Fig. 2. Schematic representation of the activation tagging T-DNA insertion sites in (A) *abs3-1D* and (B) *abs4-1D*. 35S enhancers in the activation tagging T-DNA are indicated by arrow heads. Positions and orientations of the genes flanking the activation T-DNA are indicated by arrows. (C) Northern blot analysis of At4g29140 expression levels in WT and *abs3-1D*. Equal amounts of total cellular RNAs (6 μg) extracted from 2-week-old seedlings of each genotype were separated on a formaldehyde gel and transferred onto a nylon membrane. The RNA gel blot was probed with ^{32}P-labelled full length At4g29140 cDNAs. (D) Northern blot analysis of At1g58340 expression levels in WT and *abs4-1D*. Equal amounts of total cellular RNAs (4 μg) from each genotype were loaded onto a formaldehyde gel. RNA gel blot was probed with ^{32}P-labelled full length At1g58340 cDNAs. Ethidium bromide (EB) stained RNA gels served as loading controls.

Downloaded from https://academic.oup.com/jxb/article/66/20/6327/552696 by guest on 24 April 2024

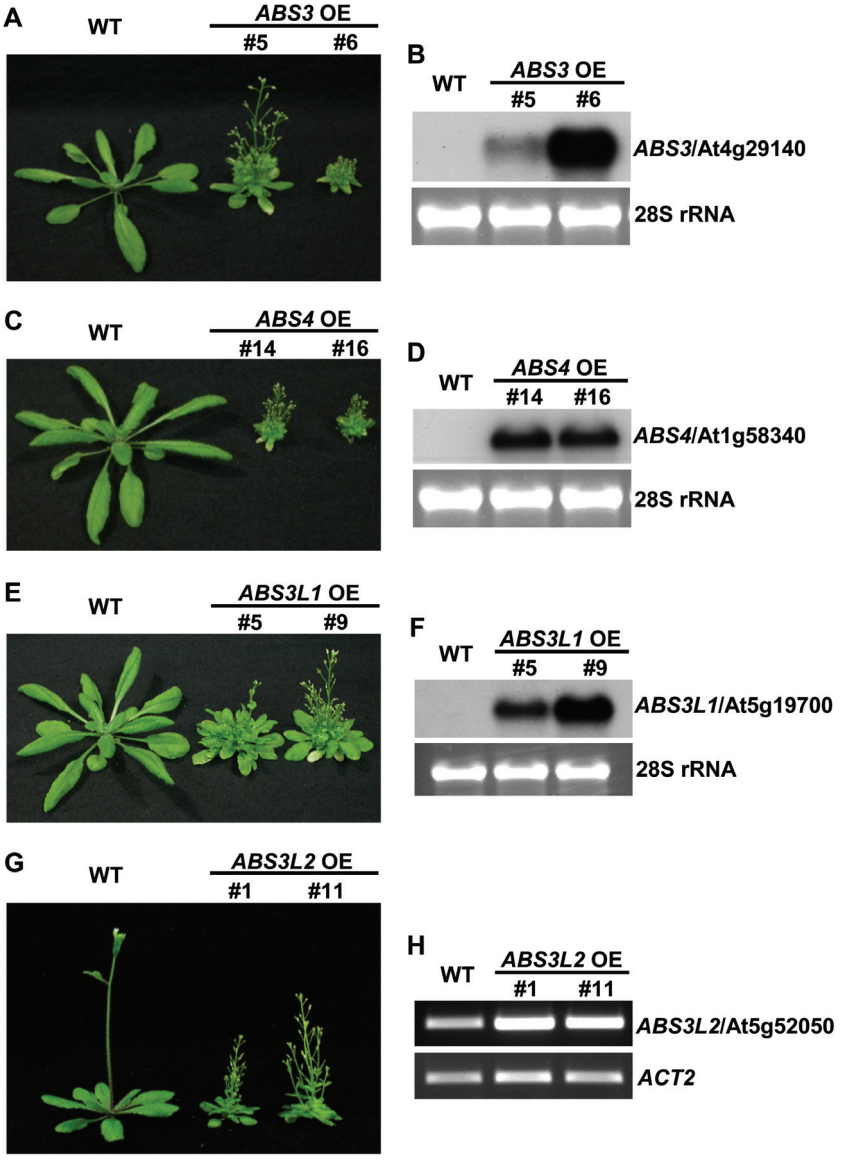

Fig. 3. Overexpression of *ABS3*, *ABS4*, *ABS3L1* and *ABS3L2* showed similar phenotypic effects. (A, C, E, G) Overall plant architectures of *ABS3*, *ABS4*, *ABS3L1* and *ABS3L2* over-expression (OE) lines. Illustrated are 4-week-old WT and representative independent OE lines of (A) *ABS3*, (C) *ABS4*, (E) *ABS3L1* and (G) *ABS3L2*. Expression level analysis of (B) *ABS3*, (D) *ABS4* and (F) *ABS3L1* using northern blot, and of (H) *ABS3L2* using semi-quantitative RT-PCR. Total cellular RNAs were extracted from the aerial parts of 2-week-old seedlings. For northern blots, equal amounts of total cellular RNAs (2 μg) were loaded on formaldehyde gels and RNA gel blots were performed as in Fig. 2C. EB-stained RNA gels served as loading controls. For semi-quantitative RT-PCR, 1 μg DNase I treated RNAs were used for synthesizing cDNA. Expression of *ACT2* gene was used as an internal control.

(*ALTERED DEVELOPMENT PROGRAM1*, Li *et al.*, 2014). At1g58340 was reported as *ZRZ* (*ZRIZI*) in a screen of enhancer trap lines (Burko *et al.*, 2011) and as *BCD1* (*BUSH-AND-CHLOROTIC-DWARF 1*) in an activation tagging screen (Seo *et al.*, 2012).

We next asked whether the over-expression of other *MATE* transporter genes in the same phylogenetic clade as *ABS3* and *ABS4* can have similar phenotypic effects. Two additional *MATE* genes that we named *ABS3-Like1* (*ABS3L1*, At5g19700) and *ABS3L2* (At5g52050), which are closely related to *ABS3*, were chosen and OE lines of these two genes were generated. Multiple *ABS3L1* or *ABS3L2* OE lines showed enhanced leaf initiation rate, shorter petioles, more compact rosette, and increased numbers of branches, and these phenotypes closely resembled those of *ABS3* or *ABS4* OE lines (Fig. 3E, G). Northern blot or semi-quantitative RT-PCR analysis confirmed the elevated levels of *ABS3L1* or *ABS3L2* transcripts in OE lines (Fig. 3F, H). These data indicate that increased expressions of a subfamily of *MATE* transporter genes including *ABS3*, *ABS4*, *ABS3L1* and *ABS3L2* are capable of altering shoot developmental programmes in a similar manner.

ABS3, ABS4, ABS3L1 *and* ABS3L2 *have distinctive expression patterns*

To further our understanding of the roles that *ABS3*, *ABS4*, *ABS3L1* and *ABS3L2* play in development, we next looked at the tissue and developmental expression profiles of these genes. Semi-quantitative RT-PCR analysis using cDNAs

Downloaded from https://academic.oup.com/jxb/article/66/20/6327/552696 by guest on 24 April 2024

synthesized from RNAs of various tissues indicated that *ABS3* and its related *MATE* genes have diverse expression patterns (Supplementary Fig. S2). Next, promoter regions (~1.5−2 kb upstream to the start codon) of these four genes were fused with β-glucuronidase (GUS) gene and these reporter constructs were transformed into WT *Arabidopsis*. GUS activities were assayed at the T2 generation and Fig. 4 shows that these four genes had distinctive expression

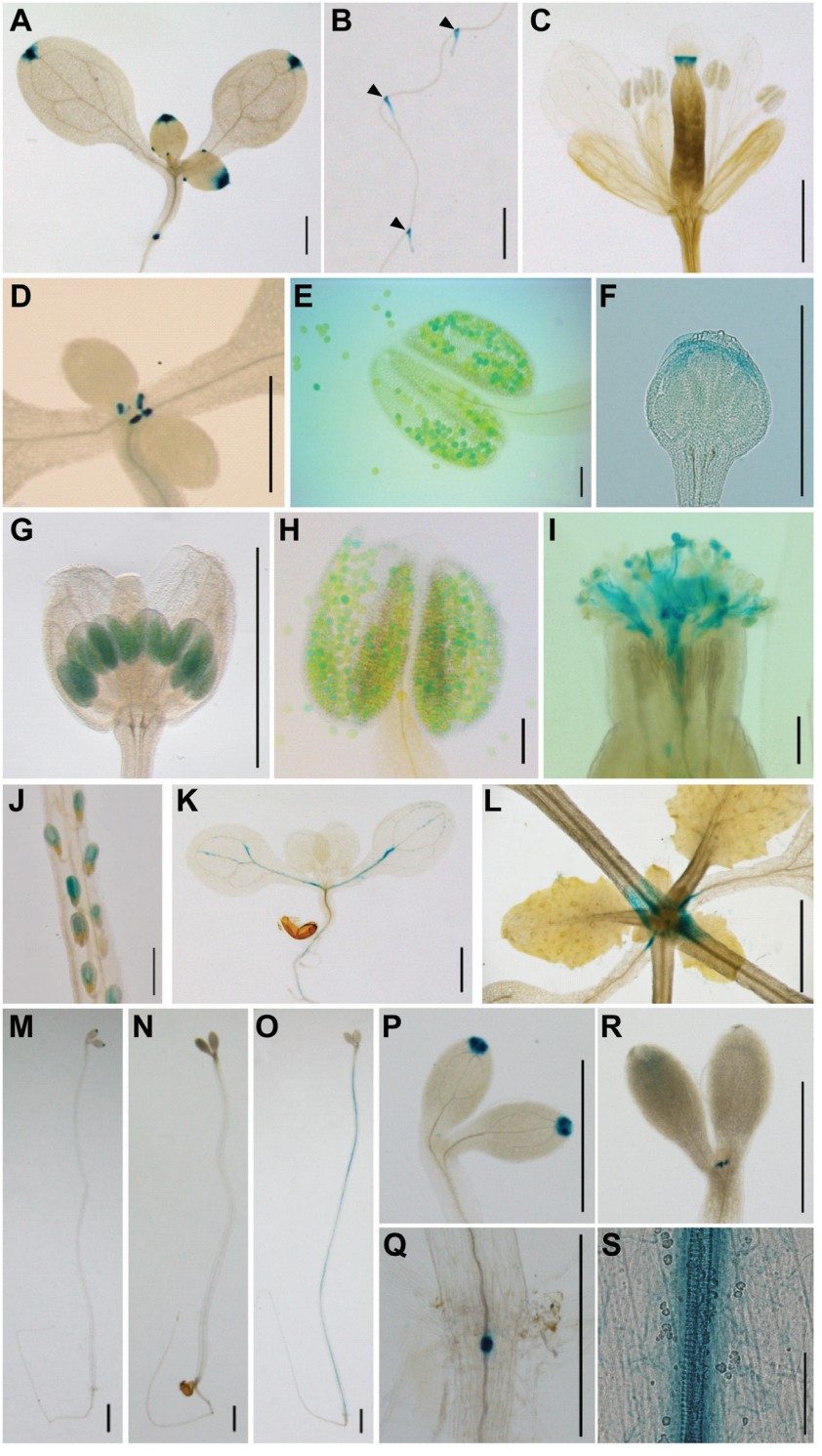

Fig. 4. Expression patterns of *ABS3*, *ABS4*, *ABS3L1* and *ABS3L2*. Expression of P_{ABS3}*::GUS* in (A) the 2-week-old seedling, (B) young lateral roots and (C) the style of the pistil. Positions of lateral roots are indicated by black arrow heads in B. Expression of P_{ABS4}*::GUS* in (D) stipules, (E) mature pollen and (F) the sepal. Expression of P_{ABS3L1}*::GUS* in (G) young anthers, (H) mature pollen, (I) germinating pollen and pollen tubes and (J) developing seeds. Expression of P_{ABS3L2}*::GUS* in (K) some vascular tissues of 6-day-old seedlings and (L) in the basal regions of leaf petioles of 3-week-old plants. Expression of (M) P_{ABS3}*::GUS*, (N) P_{ABS4}*::GUS* and (O) P_{ABS3L2}*::GUS* in 6-day-old dark-grown seedlings. Enlarged image of (P) cotyledons and (Q) the hypocotyl-root junction of the seedling shown in M. (R) Enlarged image of the shoot apical region of the seedling shown in N. (S) Enlarged image of the hypocotyl vascular tissues in the seedling shown in O. Bars: 1 mm (A–D, F, G, J–R); 100 μm (E, H, I); 50 μm (S).

Downloaded from https://academic.oup.com/jxb/article/66/20/6327/552696 by guest on 24 April 2024

patterns. In light-grown seedlings, *ABS3* was highly expressed at the junction between the hypocotyl and the root, and at the marginal areas of cotyledons and true leaves, coinciding with the locations of the hydathode (Fig. 4A). *ABS3* was also highly expressed at the basal regions of the newly emerged lateral roots (Fig. 4B). In the floral organs, *ABS3* was mostly expressed at the style of the pistil (Fig. 4C). At vegetative stages, *ABS4* was highly expressed at the stipules (Fig. 4D). At reproductive stages, *ABS4* was most highly expressed in the mature pollen (Fig. 4E). *ABS4* was also expressed in the tips of sepals (Fig. 4F). Expression of *ABS3L1* was mostly detected at reproductive stages in young anthers, in mature pollens and during pollen germination on the pistil (Fig. 4G–I). *ABS3L1* is also expressed in developing seeds (Fig. 4J). For the *ABS3L2* promoter, GUS activities were detected in the part of the veins in cotyledons of 6-day-old seedlings and the basal parts of the petioles in older plants (Fig. 4K, L).

Expressions of the *ABS3* subfamily of *MATE* genes were also examined in dark-grown seedlings (Fig. 4M–S). In 6-day-old etiolated seedlings, expression patterns of *ABS3* and *ABS4* were similar to those observed in light-grown seedlings (Fig. 4M, N, P–R). Expression of *ABS3* was restricted to the cotyledon tips and the hypocotyl-root junction (Fig. 4M, P, Q) while expression of *ABS4* was mostly found in the stipules (Fig. 4N, R). In contrast to its relative low expression level in light-grown seedlings, *ABS3L2* was highly expressed in the vascular tissues of hypocotyl in dark-grown seedlings (Fig. 4O, S). We did not detect GUS signals for *ABS3L1* in etiolated seedlings. Taken together, these data indicate that the expressions of the *ABS3* subfamily of *MATE* genes are highly regulated at different tissues and developmental stages.

ABS3, ABS4, ABS3L1 and ABS3L2 localize to the LE/PVC compartment

Previously reported *Arabidopsis* MATE transporters have been shown to be targeted to different compartments (Li *et al.*, 2002; Magalhaes *et al.*, 2007; Serrano *et al.*, 2013). To establish the sub-cellular localizations of the ABS3 subfamily of MATE transporters, we generated constructs expressing fluorescent protein tagged ABS3, ABS4, ABS3L1 and ABS3L2 and analysed the distribution patterns of these fusion proteins in *Arabidopsis* leaf protoplasts. We first determined that ABS3-GFP (GFP fused at the C-terminus of ABS3) and mCherry-ABS3 (mCherry fused at the N-terminus of ABS3) co-localized with each other, suggesting that the position of the fluorescent protein tag does not interfere with the subcellular localization of ABS3 (Supplementary Fig. S3A). Given the similar OE phenotypes, we reasoned that the ABS3 subfamily of MATE transporters might reside in the same cellular compartment. To test this, we co-expressed ABS3-GFP and ABS4-mCherry in protoplasts, and confocal microscopy revealed that GFP and mCherry signals merged well, indicating that ABS3-GFP and ABS4-mCherry are targeted to the same location (Fig. 5A, B). Co-expression of ABS3L1-GFP or ABS3L2-GFP with ABS4-mCherry yielded similar results, further indicating that these four MATE proteins share the same subcellular localization (Fig. 5C–F).

As shown in Fig. 5A–F, the ABS3 subfamily of MATE proteins localized to discrete dots in the cell, suggesting that they could be targeted to small organelles or endomembrane vesicles. We next co-expressed ABS3-GFP or ABS4-mCherry with various organelle marker proteins and found that ABS3-GFP did not co-localize with peroxisome or mitochondrion markers (Fan *et al.*, 2005; Nelson *et al.*, 2007) (Supplementary Fig. S3B, C). Nor did ABS4-mCherry co-localize with ER or tonoplast markers (Supplementary Fig. S3D, E). On the other hand, co-expression of ABS4-mCherry with markers indicating different endosome compartments revealed that ABS4-mCherry merged nicely with the LE/PVC marker GFP-SYP21 (Foresti *et al.*, 2006) (Fig. 5G, H). Moreover, ABS3-GFP also co-localized with mCherry-SYP21 (Fig. 5I, J). ABS4-mCherry did not co-localize with the Golgi marker (YFP-SYP32, Geldner *et al.*, 2009) (Fig. 5K, L) or the trans-Golgi network/early endosome (TGN/EE) marker (SYP61-GFP, Viotti *et al.*, 2010) (Fig. 5M, N). Taken together, our data demonstrate that ABS3, ABS4, ABS3L1 and ABS3L2 all likely localize to LE/PVC.

ABS3, ABS4, ABS3L1 *and* ABS3L2 *negatively regulate hypocotyl cell elongation in the light*

Over-expressions of *ABS3*, *ABS4* and *ABS3-Like* genes all resulted in reduced length of leaf petioles, suggesting that these genes might be involved in the regulation of cell elongation (Figs 1, 3). We then used the *Arabidopsis* hypocotyl as the system and tested the elongation of hypocotyl cells on medium with or without sucrose. Both *abs3-1D* and *abs4-1D* had significantly shorter hypocotyls than WT on vertical plates containing 1/2 MS medium without sucrose (Fig. 6A, C). With 1% sucrose, hypocotyl growth was promoted in all three genotypes, and *abs3-1D* and *abs4-1D* again showed significant shorter hypocotyls than WT (Fig. 6B, C). However, we did observe greater hypocotyl length differences between WT and the two mutants when sucrose was present (Fig. 6C). These results suggest that elongation of the hypocotyl was inhibited in light-grown *abs3-1D* and *abs4-1D* seedlings, regardless of the presence of sucrose. To clarify whether the shortened hypocotyls in *abs3-1D* and *abs4-1D* were due to defects in cell division or cell elongation, we examined hypocotyl epidermal cells with a con-focal microscope. As illustrated in Fig. 6D, the lengths of epidermal cells in the mid-region of the hypocotyl were shorter in *abs3-1D* or *abs4-1D* compared with those of WT. These data suggest that over-production of *ABS3* or its close homologue *ABS4* has a negative impact on hypocotyl cell elongation in light-grown seedlings.

To further establish the role of *ABS3* and *ABS3-Like MATE* genes in modulating hypocotyl cell elongation, we sought loss-of-function mutants of these genes. Insertional lines *abs3-1* (SM3_36823), *abs4-1* (SALK_067667), *abs3l1-1* (SAIL_1236_H10) and *abs3l2-1* (SALK_144096) were obtained from the Arabidopsis Resource Center (Supplementary Fig. S4A, D, G, J). The overall growth and development was not grossly altered in any of the single knockout mutant compared to WT (Supplementary Fig. S4B, E, H, K). Semi-quantitative RT-PCR showed that full-length transcripts for each of

Downloaded from https://academic.oup.com/jxb/article/66/20/6327/552696 by guest on 24 April 2024

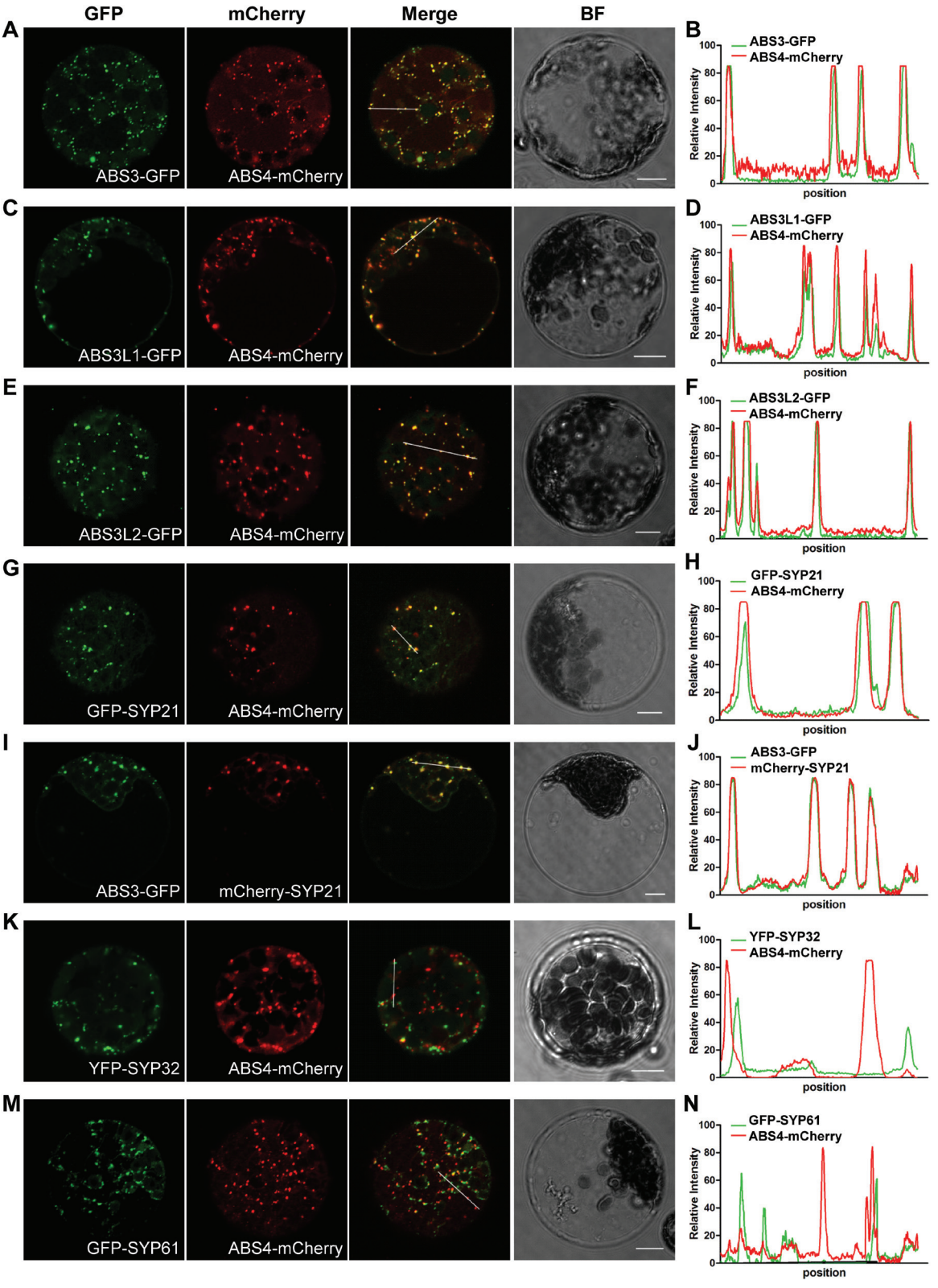

Fig. 5. Subcellular localization of ABS3, ABS4, ABS3L1 and ABS3L2. Transient co-expression of (A) ABS3-GFP, (C) ABS3L1-GFP or (E) ABS3L2-GFP with ABS4-mCherry in WT protoplasts. (G) Transient co-expression of LE/PVC marker GFP-SYP21 (Foresti *et al.*, 2006) and ABS4-mCherry in WT protoplasts. (I) Transient co-expression of ABS3-GFP and mCherry-SYP21 in WT protoplasts. (K) Transient expression of ABS4-mCherry in protoplasts isolated from transgenic lines stably expressing Golgi marker YFP-SYP32 (Geldner *et al.*, 2009). (M) Transient co-expression of TGN/EE marker GFP-SYP61 (Viotti *et al.*, 2010) and ABS4-mCherry in WT protoplasts. GFP or YFP fluorescent signals were shown in the 'GFP' column; mCherry fluorescent signals were shown in the 'mCherry' column; merged images of 'GFP' and 'mCherry' channels were shown in the 'Merge' column; bright field images of protoplasts were shown in the 'BF' column. Bars: 10 μm. (B, D, F, H, J, L, N) Co-localization analysis plots for merged images in A, C, E, G, I, K and M, respectively. Plots were generated by tracking the relative intensities of GFP/YFP and mCherry fluorescent signals marked by 'white lines' in merged images using the 'plot profile' function of ImageJ.

Downloaded from https://academic.oup.com/jxb/article/66/20/6327/552696 by guest on 24 April 2024

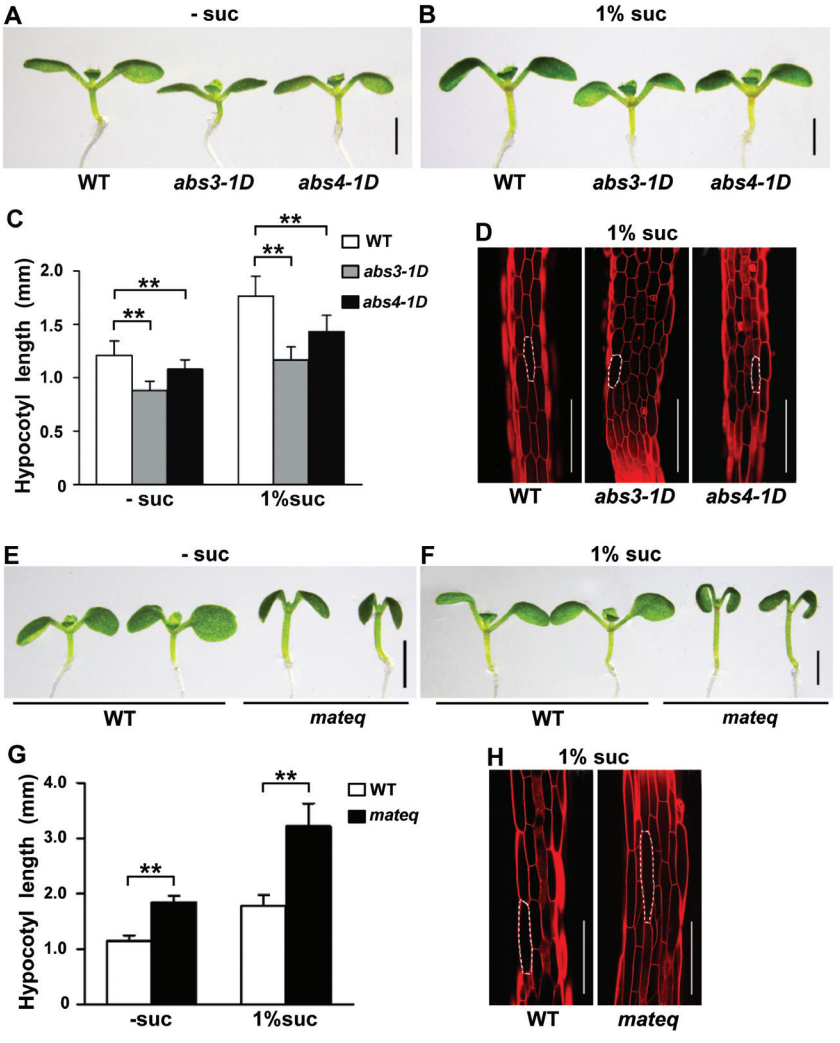

Fig. 6. Hypocotyl phenotypes of light-grown *abs3-1D*, *abs4-1D* and *mateq*. Overall plant morphologies of 7-day-old WT, *abs3-1D* and *abs4-1D* seedlings grown on 1/2 MS medium with no sucrose (A) or with 1% sucrose (B) under constant light. Bars, 1 mm. (C) Average hypocotyl length of light-grown 7-day-old WT, *abs3-1D* and *abs4-1D* grown on 1/2 MS medium with no sucrose or with 1% sucrose. Data were presented as mean ± standard deviation (s.d.) and analysed using Student's *t*-test ($n \geq 30$; **, $P < 0.01$). (D) Comparison of hypocotyl epidermal cell elongation in light-grown 7-day-old WT, *abs3-1D* and *abs4-1D* grown on 1/2 MS medium with 1% sucrose. Seedlings were stained by PI and outlines of the hypocotyl epidermal cells were captured via confocal microscopy. Illustrated are epidermal cells in the middle part of the hypocotyl. Boundaries of one representative hypocotyl epidermal cell of each genotype were traced with white dashed lines. Bars, 200 μm. Overall plant morphologies of 7-day-old wild type and *mateq* seedlings grown on 1/2 MS medium with no sucrose (E) or with 1% sucrose (F) under constant light. Bars, 1 mm. (G) Average hypocotyl length of light-grown 7-day-old WT and *mateq* grown on 1/2 MS medium with no sucrose or with 1% sucrose. Data were presented as mean ±s.d. and analysed as in C ($n \geq 30$; **, $P < 0.01$). (H) Comparison of hypocotyl epidermal cell elongation in light-grown 7-day-old WT and *mateq* grown on 1/2 MS medium with 1% sucrose. Hypocotyl epidermal cells were examined as in D. Bars, 200 μm.

the *MATE* genes were not detectable in the corresponding homozygous insertional lines (Supplementary Fig. S4C, F, I, L). However, careful examination showed that under continuous light, the hypocotyls of *abs3-1* seedlings were slightly, yet significantly, longer than that of WT on medium with or without 1% sucrose (Supplementary Fig. S5A–C). The elongation of hypocotyl epidermal cells were slightly enhanced in *abs3-1* compared to that of WT (Supplementary Fig. S5D).

Considering that weak or lack of phenotypes often indicates the existence of functional redundancy, we generated higher order mutants of these *MATE* genes. One-week-old light-grown *abs3-1 abs4-1 abs3l1-1 abs3l2-1* quadruple mutant (*mateq*) showed a more pronounced long hypocotyl phenotype compared to that of WT, and hypocotyl epidermal cells were also more elongated in *mateq* (Fig. 6E–H). Interestingly, the difference in hypocotyl lengths between WT and *mateq* was also more pronounced when 1% sucrose was included in the medium, suggesting that *mateq* may be more sensitive to the effect of sucrose when grown in the light (Fig. 6E–G). To validate that the long hypocotyl phenotype of the *mateq* mutant was a direct consequence of the lack of the four *MATE* genes, we transformed *mateq* mutants with 35S-driven *ABS3* cDNA. In T1 and T2 generations, the elongated hypocotyl of the *mateq* mutant was reversed to WT level or even shorter in multiple lines, suggesting that *ABS3* activity can complement the enhanced hypocotyl growth phenotype of the *mateq* mutant (Supplementary Fig. S6). Taken together, these data indicate that *ABS3* and *ABS3-Like MATE* genes negatively regulate hypocotyl cell elongation in light-grown seedlings.

Downloaded from https://academic.oup.com/jxb/article/66/20/6327/552696 by guest on 24 April 2024

Over-expression of ABS3, ABS4, ABS3L1 *or* ABS3L2 *leads to de-etiolation in the dark*

Given that *ABS3* and *ABS3-Like* genes are involved in regulating hypocotyl growth in light-grown seedlings, we next tested whether this group of *MATE* genes also participates in the regulation of hypocotyl growth in the dark. When grown under darkness for 6 d on medium with no sucrose, both gain-of-function mutants *abs3-1D* and *abs4-1D* displayed inhibited hypocotyl elongation (Fig. 7A, M; Supplementary Fig. S7A, M). On the other hand, with 1% sucrose in the medium, WT hypocotyl length was similar to that of WT without sucrose, but the average hypocotyl lengths of *abs3-1D* and *abs4-1D* were increased to WT length (Fig. 7D, M; Supplementary Fig. S7D, M). Cotyledons of WT, *abs3-1D* and *abs4-1D* remained closed on either type of the medium after 6 d in the dark (Fig. 7B, C, E, F; Supplementary Fig. S7B, C, E, F). These data suggest that *ABS3* and *ABS4* are potential negative regulators of hypocotyl elongation in the dark, and the presence of sucrose effectively complemented the hypocotyl elongation defects of *abs3-1D* and *abs4-1D*.

We next tested the responses of WT, *abs3-1D* and *abs4-1D* to prolonged dark treatment. Both *abs3-1D* and *abs4-1D* showed a shorter hypocotyl length compared to that of WT when growing on medium with or without sucrose after 20 days of dark growth (Fig. 7G, J, M; Supplementary S7G, J, M). The addition of sucrose promoted hypocotyl elongation in WT, *abs3-1D* and *abs4-1D* and the effect of sucrose

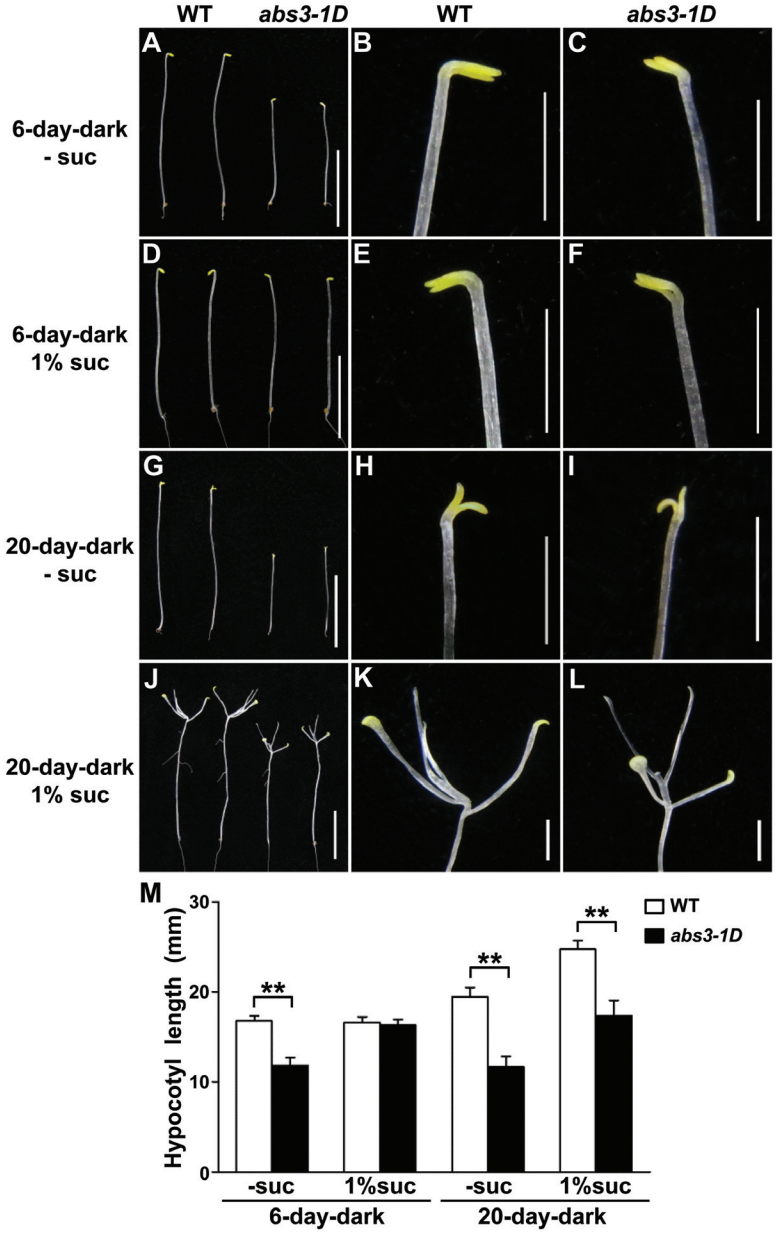

Fig. 7. De-etiolation phenotypes of dark-grown *abs3-1D.* Overall seedling morphologies of wild type and *abs3-1D* grown in the dark for 6 d (A, D) or 20 d (G, J) on 1/2 MS medium with no sucrose (A, G) or with 1% sucrose (D, J). Bars, 10 mm. (B–C, E–F, H–I, K–L) Apical parts of plants shown in A, D, G and J, respectively. Bars, 2 mm. (M) Average hypocotyl length of WT and *abs3-1D* grown in the dark for 6 d or 20 d on 1/2 MS medium with no sucrose or with 1% sucrose. Data were presented as mean ± s.d. and statistical comparisons were performed as in Fig. 6C ($n \geq 30$; **, $P < 0.01$).

Downloaded from https://academic.oup.com/jxb/article/66/20/6327/552696 by guest on 24 April 2024

was more pronounced for *abs3-1D* and *abs4-1D* (Fig. 7J, M; Supplementary S7J, M). Sucrose also promoted cotyledon opening and differentiation of apical meristem in WT, *abs3-1D* and *abs4-1D* (Fig. 7H, I, K, L; Supplementary S7H, I, K, L). These data support the conclusion of the 6-day dark treatment.

To further establish the effects of over-expression of *ABS3* subfamily *MATE* transporter genes on dark-grown seedlings, we compared the growth of 35S promoter driven *ABS3*, *ABS4*, *ABS3L1* and *ABS3L2* OE lines with WT in the dark for 6 d or 20 d. In the dark, the hypocotyl elongations in *ABS3* OE lines were strongly inhibited compared to that of WT regardless of the presence of sucrose in the medium after 6 d or 20 d (Fig. 8A, E, I, M). Furthermore, multiple *ABS3* OE lines showed additional de-etiolation phenotypes of open and elongated cotyledons on medium with or without sucrose after 6 d of dark growth (Fig. 8B–D, F–H). After 20 d of dark growth, both WT and *ABS3* OE lines had opened cotyledons (Fig. 8I–P). On plates without sucrose, no differentiation of apical meristem was observed (Fig. 8I–L). With 1% sucrose, the differentiation of true leaves can be observed in WT etiolated seedlings after 20 d, but *ABS3* OE lines in general showed a more prominent development of true leaves (Fig. 8M–P). Examination of the hypocotyl epidermal cells confirmed that cell elongation was strongly suppressed in *ABS3* OE lines compared to that of WT (Fig. 8Q, R). Similar to *ABS3* OE lines, OE lines of other *ABS3* subfamily *MATE* genes, including *ABS4*, *ABS3L1* and *ABS3L2*, also displayed a dramatic inhibition of hypocotyl elongation and characteristics of photomorphogenesis in the dark (Supplementary Figs S8–10).

Next, we asked whether the de-etiolation phenotypes of *ABS3* OE lines were accompanied with altered plastid development in the dark. Cotyledons of 6-day-old dark-grown seedlings grown on the medium with or without 1% sucrose were examined with a transmission electron microscope. Under either growth conditions, WT mesophyll cells contained typical etioplasts containing the characteristic prolamellar body (PLB) structure, while partially differentiated plastids with thylakoid-like membranes were identified in cotyledon mesophyll cells of *ABS3* OE#5 (Fig. 8S, T). These data further demonstrate that over-production of *ABS3* and *ABS3-Like MATE* genes is capable of negatively regulating cell elongation in the dark and producing de-etiolation phenotypes that resemble the well-known de-etiolation phenotypes of the *det/cop/fus* mutants (Chory *et al.*, 1989; Deng *et al.*, 1991; Castle and Meinke, 1994; Miséra *et al.*, 1994).

Loss of ABS3 subfamily MATE transporters leads to enhanced hypocotyl elongation in the dark

We next tested the impact of loss-of-function mutations of *ABS3*, *ABS4*, *ABS3L1* and *ABS3L2* on hypocotyl elongation in the dark. *mateq* mutants behaved in a similar manner with WT over short periods (6 d) of dark growth on medium with or without 1% sucrose (Fig. 9A–F, M). After prolonged dark treatment (20 d), hypocotyl elongation and cotyledon openness were still comparable for WT and *mateq* when no sucrose was present in the medium (Fig. 9G–I, M). However, on medium with 1% sucrose, although both WT and *mateq* showed a general enhanced elongation of hypocotyls compared with that on a no-sucrose medium, *mateq* appeared to show a more dramatic response to sucrose as its hypocotyls were significantly longer than those of WT (Fig. 9J, M). Examination of PI-stained hypocotyls further confirmed that *mateq* had more elongated hypocotyl epidermal cells compared to those of WT when grown in darkness for 20 d with 1% sucrose (Fig. 9N). In addition, while the presence of sucrose in the medium promoted the differentiation of true leaves in WT, the true leaves of *mateq* were less developed (Fig. 9K, L). These observations suggest that the *mateq* mutant has stronger etiolation responses than WT under prolonged darkness in the presence of sucrose. Taken together, we conclude that *ABS3* and *ABS3-Like MATE* genes are likely negative regulators of skotomorphogenesis when sucrose is present.

ABS3 *and* ABS4 *genetically interact with* PHYB

To further explore the mechanism of *ABS3*′s involvement in regulating plant growth, we carried out screens for genetic modifiers of *abs3-1D* with ethylmethane sulfonate (EMS) mutagenesis. One suppressor line, designated *F07-08*, with longer leaf petioles was isolated (Fig. 10A). Interestingly, the *F07-08* single mutant showed an exaggerated elongation of hypocotyls and petioles, while the hypocotyl length of the *F07-08* double mutant was intermediate between the parent mutants (Fig. 10A–C). Furthermore, the hypocotyl cell elongation defects of *abs3-1D* was effectively reversed by the presence of *F07-08* single mutation, and the *F07-08* single mutant itself exhibited an exaggerated elongation of hypocotyl cells (Fig. 10D). Overall, the phenotypes of the *F07-08* single mutants are reminiscent of the classic *long hypocotyl3* (*hy3*) mutant, which is defective in the photoreceptor phytochrome B gene *PHYB*. To verify if the *F07-08* single mutant is an allele of *PHYB*, we sequenced the genomic region of *PHYB* in *F07-08* and identified a G-to-A mutation that converts a tryptophan codon (W563) to a stop codon (Fig. 10E). Thus we concluded that the *F07-08* single mutant represents a mutant allele of *PHYB*.

We next determined the genetic interaction between *abs4-1D* and the *F07-08* single mutant, and found that the *F07-08* single mutant was also able to reverse the hypocotyl cell elongation defect of *abs4-1D* (Supplementary Fig. S11). Next, we introduced 35S-driven *ABS3* or *ABS4* cDNA into *phyB-1* background and found markedly reduced hypocotyl elongation in multiple transgenic lines, further confirming the genetic interaction between *ABS3*, *ABS4* and *PHYB* (Supplementary Fig. S12). These results further validated the role of ABS3 and ABS4 as negative regulators of hypocotyl cell elongation.

Discussion

Cell elongation is a fundamental process in developmental biology and higher plants have to integrate multiple signalling pathways to exercise precise control over cell

Downloaded from https://academic.oup.com/jxb/article/66/20/6327/552696 by guest on 24 April 2024

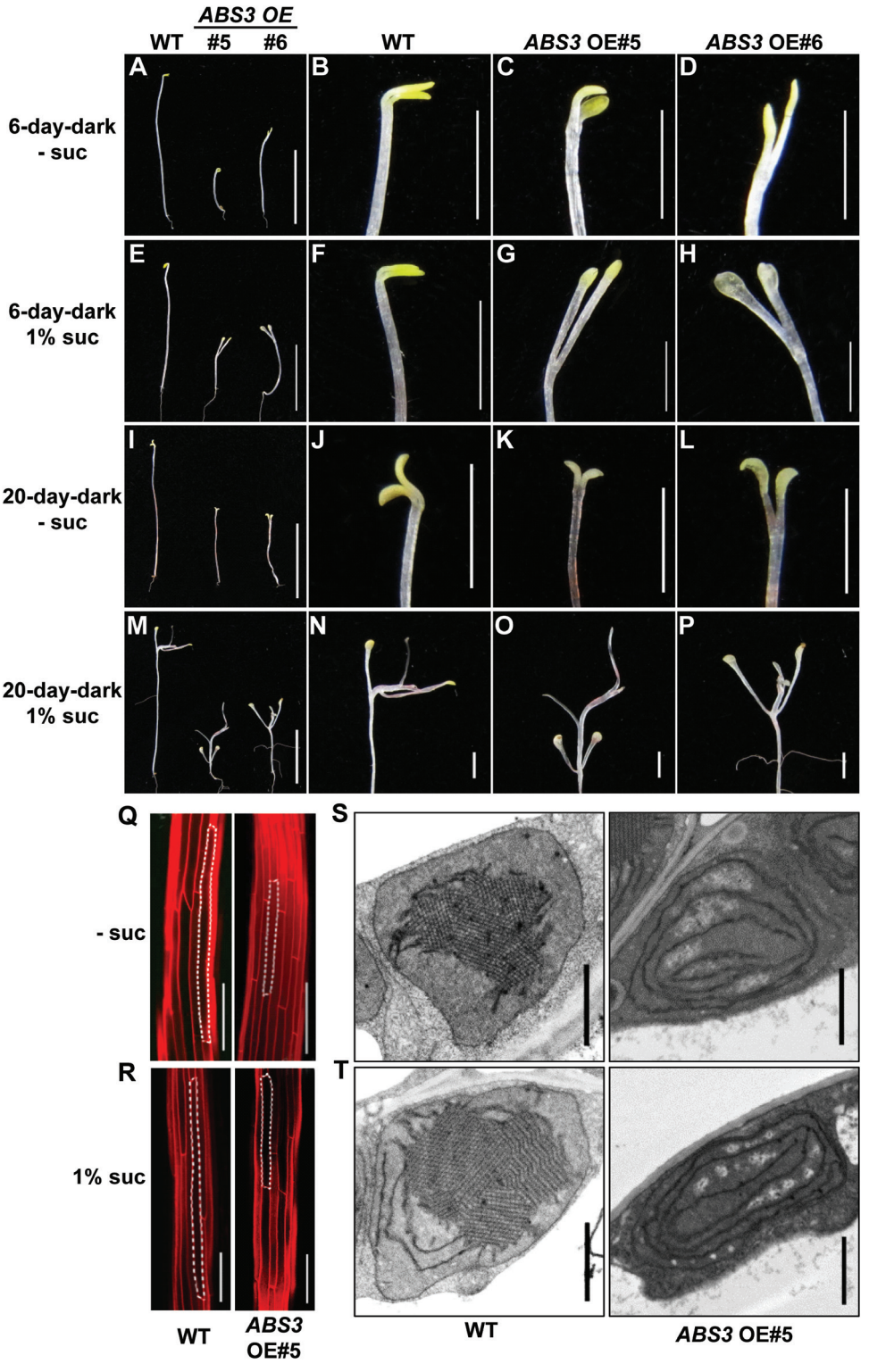

Fig. 8. De-etiolation phenotypes of dark-grown *ABS3* OE lines. Overall seedling morphologies of WT and two independent *ABS3* OE lines (OE#5 and OE#6) grown in the dark for 6 days (A, E) or 20 days (I, M) on 1/2 MS medium without sucrose (A, I) or with 1% sucrose (E, M). Bars, 10 mm. (B–D, F–H, J–L, N–P) Apical parts of plants shown in A, E, I and M, respectively. Bars, 2 mm. (Q, R) Comparison of hypocotyl epidermal cell elongation in WT and *ABS3* OE#5 grown on 1/2 MS medium without sucrose (Q) or with 1% sucrose (R) in the dark for 6 d. Hypocotyl epidermal cells were examined as in Fig. 6D. Bars, 200 μm. Ultrastructure of plastids in 6-day-old dark-grown WT or *ABS3* OE#5 cotyledon mesophyll cells: plants were grown on 1/2 MS medium without sucrose (S) or with 1% sucrose (T). Bars: 1 μm.

elongation to ensure proper plant growth and development. Environmental cues including light exert profound impacts on plant cell elongation (Leyser and Day, 2009). In the presence of light, photoreceptors such as phytochrome B act to initiate photomorphogenesis and the inhibition of hypocotyl cell elongation is a key component of this process (Arsovski *et al.*, 2012). In the dark, however, plant hypocotyls undergo rapid elongation, as part of the skotomorphogenesis (Chory

Downloaded from https://academic.oup.com/jxb/article/66/20/6327/552696 by guest on 24 April 2024

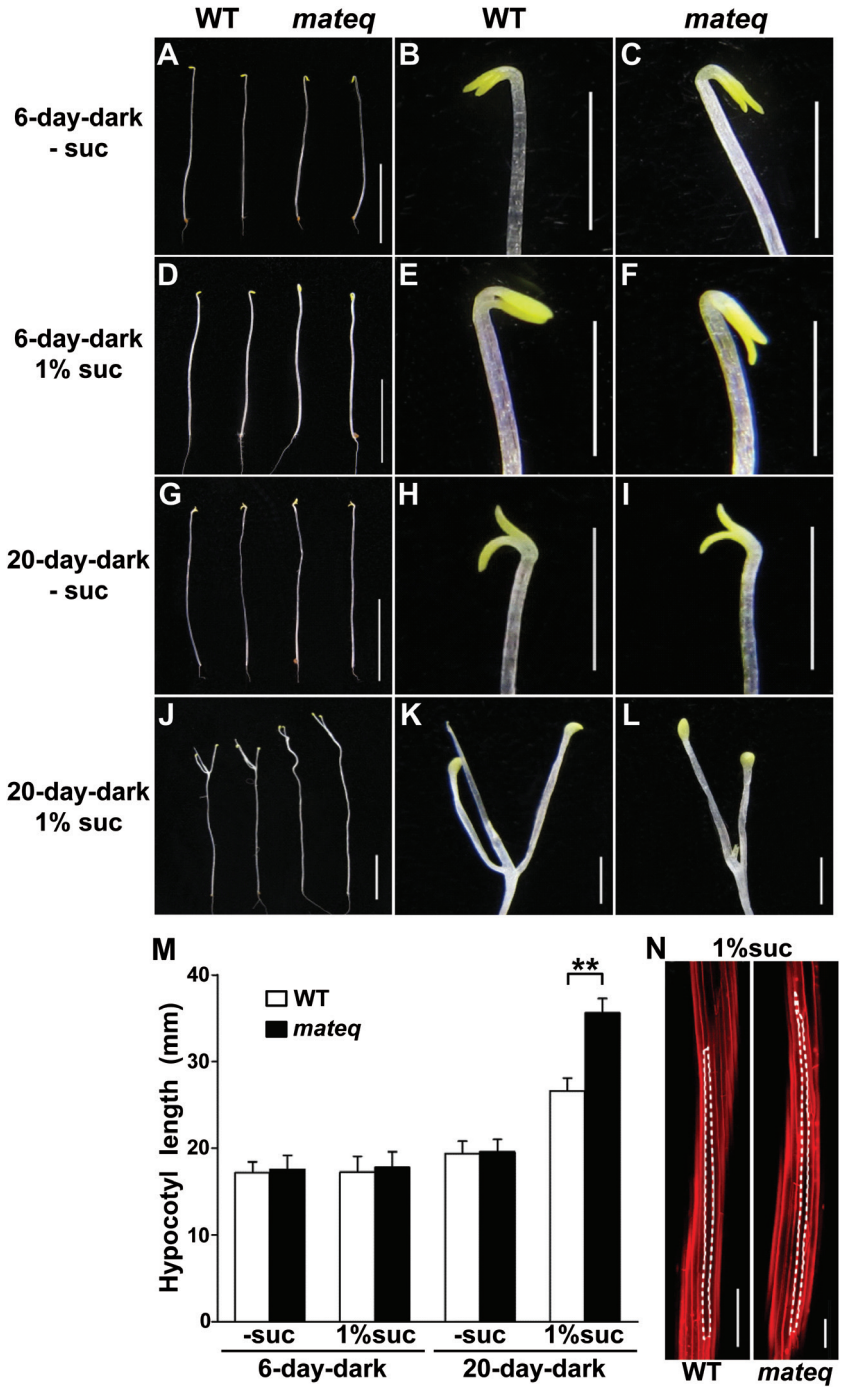

Fig. 9. Phenotypes of dark-grown *mateq* mutant. Overall seedling morphologies of WT and *mateq* grown in the dark for 6 d (A, D) or 20 d (G, J) on 1/2 MS medium without sucrose (A, G) or with 1% sucrose (D, J). Bars, 10 mm. (B–C, E–F, H–I, K–L) Apical parts of plants shown in A, D, G and J, respectively. Bars, 2 mm. (M) Average hypocotyl length of WT and *abs3-1D* grown in the dark for 6 d or 20 d on 1/2 MS medium with no sucrose or with 1% sucrose. Data were presented as mean ±s.d. and statistical comparisons were performed as in Fig. 6C ($n \geq 30$; **, $P < 0.01$). (N) Comparison of hypocotyl epidermal cell elongation of WT and *mateq* grown in the dark for 20 d on 1/2 MS medium with 1% sucrose. Hypocotyl epidermal cells were examined as in Fig. 6D. Bars, 200 μm.

et al., 1989). Exploiting these traits, researchers have identified mutants such as the *hy* and *det/cop/fus* mutants that display altered light or dark hypocotyl cell elongation growth patterns, and the cloning of these genes led to our current understanding of the framework for plant light and dark morphogenesis (Chory *et al.*, 1989; Deng *et al.*, 1991; Castle and Meinke, 1994; Miséra *et al.*, 1994). In addition, plant hormones including gibberellins, brassinosteroids, auxin and cytokinins also play critical roles in regulating cell elongation (Chory *et al.*, 1994; Li *et al.*, 1996; Feng *et al.*, 2008; Halliday *et al.*, 2009; Oh *et al.*, 2012). At the structural level, defects such as those in cytoskeleton and cell wall synthesis can profoundly affect plant cell elongation (Fagard *et al.*, 2000; Pelletier *et al.*, 2010).

Mechanisms of multidrug resistance have drawn considerable interest as humans face the ever increasing challenges

Downloaded from https://academic.oup.com/jxb/article/66/20/6327/552696 by guest on 24 April 2024

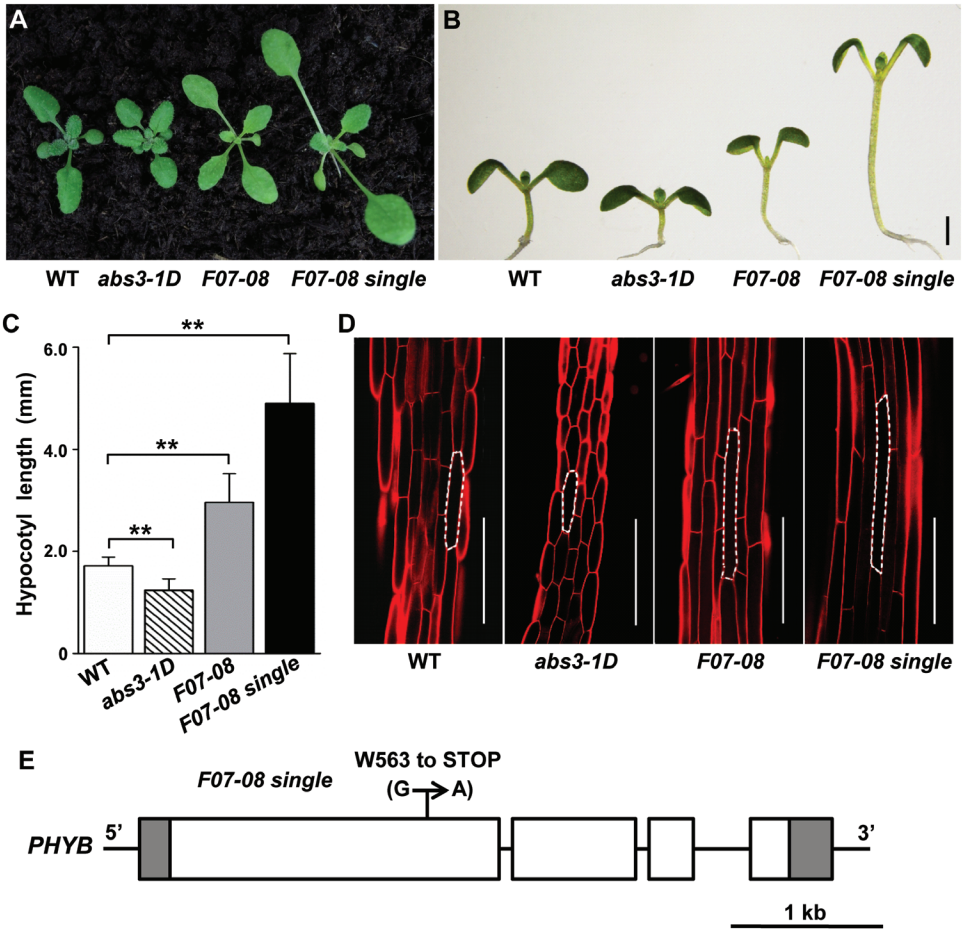

Fig. 10. Genetic interaction between *abs3-1D* and *phyB* mutant. (A) Overall plant morphologies of 2-week-old WT, *abs3-1D*, *F07-08* and *F07-08 single* mutant grown on the soil. (B) Hypocotyl phenotypes of 7-day-old WT, *abs3-1D*, *F07-08* and *F07-08 single* mutant grown on 1/2 MS medium with 1% sucrose under constant light. Bar, 1 mm. (C) Average hypocotyl lengths of WT, *abs3-1D*, *F07-08* and *F07-08 single* mutant grown under the same conditions as in B. Data were presented as mean ±s.d. and analysed as in Fig. 6C ($n \geq 30$; **, $P<0.01$). (D) Comparison of hypocotyl epidermal cell elongation in plants shown in B. Epidermal cells were examined as in Fig. 6D. Bars, 200 μm. (E) Schematic representation of the mutation site identified in *F07-08*. In the *PHYB* gene model, exons and introns were represented by boxes and solid lines, respectively. 5′ and 3′ untranslated regions (UTRs) were represented by shaded boxes.

of multidrug resistant bacteria (Monk and Goffeau, 2008; Nikaido, 2009). One common strategy for bacterial drug resistance is through efflux transporters, which are capable of mediating the efflux of antibiotics, and several efflux transporter families including the MATE family have been identified (Nikaido, 2009). The canonical bacterial MATE family transporter NorM can transport a host of small molecules including antibiotics and is involved in multiple cellular processes (Morita *et al.*, 1998). An expansion of the MATE family of transporters is seen in *A. thaliana* and at least 56 putative *MATE* family transporter genes can be identified (Li *et al.*, 2002). The presence of a large gene family suggests a certain degree of gene functional redundancy and also implies potential differential gene expression regulations through distinct tissue expression patterns or protein subcellular localizations.

In this report, through activation tagging mutant screens and the isolation of gain-of-function *abs3-1D* and *abs4-1D* mutants, we established that the over-expressions of four closely related *Arabidopsis MATE* transporter genes *ABS3*, *ABS4*, *ABS3L1* and *ABS3L2* lead to pleiotropic developmental phenotypes including an increased initiation rate of leaves and auxiliary buds, and early flowering (Figs 1, 3). We further established that these four *MATE* transporter genes are regulators of hypocotyl cell elongation in light- and dark-grown seedlings. In the light, the increased expression of *ABS3* or *ABS4* leads to an inhibition of hypocotyl elongation while the simultaneous disruption of *ABS3*, *ABS4*, *ABS3L1* and *ABS3L2* in *mateq* mutants gives rise to a moderate 'long hypocotyl' phenotype (Fig. 6). We determined that the hypocotyl elongation defects likely occurred at the level of cell elongation and our results suggest genetically that these four *MATE* genes are likely to be negative regulators of hypocotyl cell elongation. The negative effect of these genes on hypocotyl elongation is not dependent on light, as gain-of-function mutants of *ABS3* and its related *MATE* genes also showed inhibited hypocotyl cell elongation and constitutive photomorphogenesis in the dark, while the *mateq* quadruple knockout mutant showed enhanced hypocotyl cell elongation in the dark (Figs 7–9; Supplementary Figs S7–S10). Our genetic work further established that *ABS3* or *ABS4* overexpression can partially rescue the long hypocotyl phenotype

Downloaded from https://academic.oup.com/jxb/article/66/20/6327/552696 by guest on 24 April 2024

caused by mutations in the *PHYB* gene, suggesting a genetic link between these *MATE* genes and the photoreceptor gene *PHYB* (Fig. 10; Supplementary Fig. S11). It is interesting to note that 35S driven *ABS3* or *ABS4* over-expression lines can reverse *phyB-1* hypocotyl length to almost WT level (Supplementary Fig. S12), suggesting that *ABS3* or *ABS4* alone, when ectopically expressed, can fully compensate the lack of photoreceptor phytochrome B in terms of hypocotyl growth. It is thus possible that ABS3 and its related transporters may be downstream executors of phytochrome B's inhibition on hypocotyl elongation. Alternatively, they may represent potential new regulators of hypocotyl cell elongation in pathways that do not involve phytochrome B.

Our findings with the four *MATE* transporter genes suggest that the biological functions of these transporters are likely related, as over-expressions of individual genes all led to similar development alterations both in the light and in the dark, particularly the inhibition on hypocotyl cell elongation. Conversely, the functional redundancy can also be seen through the loss-of-function mutants as only higher order mutants exhibited strong phenotypes. Our results indicate that these transporter genes have clearly acquired different tissue-specific expression profiles and this may represent one form of gene diversification during the evolution of *MATE* family genes (Fig. 4). In bacteria, MATE transporters locate in the plasma membrane while in plants transporters have also shown diverse sub-cellular localizations, including in the plasma membrane, tonoplast and chloroplast envelope (Li *et al.*, 2002; Magalhaes *et al.*, 2007; Nikaido, 2009; Serrano *et al.*, 2013). We showed that the four MATE transporters we investigated all localize to the LE/PVC compartment of the plant endomembrane system (Fig. 5), in agreement with the previous notion that ABS3 may be localized to endomembrane systems (Li *et al.*, 2014). Recently, the plant endomembrane system, including the Golgi apparatus, ER and endosomes, has been recognized as an important player in many developmental processes including cell elongation (Geldner *et al.*, 2007; Spitzer *et al.*, 2009; Gendre *et al.*, 2011; Ding *et al.*, 2012). Our data established that the *Arabidopsis MATE* family of transporter genes, *ABS3*, *ABS4*, *ABS3L1* and *ABS3L2*, can regulate cell elongation, further supporting the notion of a close functional relationship between the plant endomembrane system and cell elongation. Our data also implicated sucrose in the regulation of hypocotyl elongation by these *MATE* genes, especially in the dark, as the cell elongation defects of *abs3-1D* and *abs4-1D* etiolated seedlings can be rescued by exogenously applied sucrose and the enhanced cell elongation of the *mateq* mutant in the dark required the presence of sucrose (Figs 7, 9).

In previous studies, *ABS3* was identified as *ADS1* and was implicated in plant immune responses (Sun *et al.*, 2011). *ABS4* has also been identified through two independent activation tagging screens as *ZRZ* and *BCD1* and has been shown to be involved in plant organ initiation and the maintenance of iron homeostasis (Burko *et al.*, 2011; Seo *et al.*, 2012). In a recent report, *ABS3* was isolated again as *ADP1*, based on the altered plant architecture in an activation tagged mutant allele *adp1-1D* (Li *et al.*, 2014). It has been shown that biosynthesis of the plant hormone auxin may be disturbed in meristems of *adp1-1D* (Li *et al.*, 2014). However, our findings of the involvement of *ABS3* and three related *MATE* genes in regulating hypocotyl cell elongation suggest that these *MATE* genes also play important roles outside of meristems. The defects we observed with gain-of-function and loss-of-functions alleles of these four genes are not entirely correlated with a simple change of auxin level. For example, the over-production of auxin in the *yucca* mutant leads to elongated hypocotyls in the light and shortened hypocotyls in the dark (Zhao *et al.*, 2001). Our quadruple *mateq* mutants showed long hypocotyls in the light, similar to the auxin over-accumulating *yucca* mutant, however the dark phenotype of elongated hypocotyls of the quadruple mutants is opposite to the shorter hypocotyls of *yucca* mutants (Zhao *et al.*, 2001). Apparently the relationship between the *ABS3* subfamily *MATE* genes and auxin need to be further investigated. It is interesting to note that *abs3-1D* and *abs4-1D*, as well as all previously reported mutant alleles of *ABS3* or *ABS4,* were all isolated in activation tagging screens, further demonstrating the utility of gain-of-function screens in unmasking gene redundancy.

One of the major challenges for plant MATE transporters is the determination of their exact transport substrates. At present, the best characterized case is TT12, which sits in the tonoplast membrane and may carry out glycosylated flavan-3-ol transport in the flavonoid biosynthetic pathway (Debeaujon *et al.*, 2001; Marinova *et al.*, 2007). For ABS3, ABS4, ABS3L1 and ABS3L2, it is highly likely that they normally carry out the transportation of a small molecule (or small molecules) across the LE/PVC membrane. Given the clear involvement of these *MATE* transporter genes in regulating hypocotyl cell elongation and the fact that these genes are also linked with iron homeostasis, pathogen responses and organogenesis, it is likely that the homeostasis of this small molecule(s) in the plant cell is important for many aspects of plant growth and development and may act as a plant growth regulator through its direct or indirect actions.

Supplementary data

Supplementary data are available at *JXB* online.

Supplementary Table S1. Primers used in this study.

Supplementary Table S2. Summary of organelle markers used in this study.

Supplementary Fig. S1. Co-segregation analysis of *abs3-1D* and *abs4-1D*.

Supplementary Fig. S2. Tissue expression patterns of *ABS3*, *ABS4*, *ABS3L1* and *ABS3L2* analysed by semi-quantitative RT-PCR.

Supplementary Fig. S3. Transient co-expression of ABS3-GFP or ABS4-mCherry with various organelle markers in *Arabidopsis* leaf protoplasts.

Supplementary Fig. S4. Isolation of loss-of-function mutants of *ABS3*, *ABS4*, *ABS3L1* and *ABS3L2*.

Supplementary Fig. S5. Hypocotyl phenotypes of light-grown *abs3-1* mutant.

Downloaded from https://academic.oup.com/jxb/article/66/20/6327/552696 by guest on 24 April 2024

Supplementary Fig. S6. Overexpression of *ABS3* complements the hypocotyl phenotype of *mateq* quadruple mutant.

Supplementary Fig. S7. De-etiolation phenotypes of dark-grown *abs4-1D*.

Supplementary Fig. S8. De-etiolation phenotypes of dark-grown *ABS4* OE lines.

Supplementary Fig. S9. De-etiolation phenotypes of dark-grown *ABS3L1* OE lines.

Supplementary Fig. S10. De-etiolation phenotypes of dark-grown *ABS3L2* OE lines.

Supplementary Fig. S11. Genetic interaction between *abs4-1D* and *phyB* mutant.

Supplementary Fig. S12. Overexpression of *ABS3* or *ABS4* rescues long hypocotyl phenotype of *phyB-1*.

Acknowledgements

This work was supported by funding from the National Natural Science Foundation of China (31071073, 31170219 to FY, 31100864 to XL and 31300988 to YQ) and by grants from the Natural Science Foundation of Shaanxi Province, China (2012JQ3015 to JS).

References

Arsovski AA Galstyan A, Guseman JM, Nemhauser JL. 2012. Photomorphogenesis. *The Arabidopsis Book* **10,** e0147.

Burko Y, Geva Y, Refael-Cohen A, Shleizer-Burko S, Shani E, Berger Y, Halon E, Chuck G, Moshelion M, Ori N. 2011. From organelle to organ, ZRIZI MATE-type transporter that enhances organ initiation. *Plant & Cell Physiology* **52,** 518–527.

Castle LA, Meinke DW. 1994. A *FUSCA* gene of *Arabidopsis* encodes a novel protein essential for plant development. *The Plant Cell* **6,** 25–41.

Chen M, Chory J, Fankhauser C. 2004. Light signal transduction in higher plants. *Annual Review of Genetics* **38,** 87–117.

Chory J, Peto C, Feinbaum R, Pratt L, Ausubel F. 1989. *Arabidopsis thaliana* mutant that develops as a light-grown plant in the absence of light. *Cell* **58,** 991–999.

Chory J, Reinecke D, Sim S, Washburn T, Brenner M. 1994. A Role for cytokinins in de-etiolation in *Arabidopsis*. *Plant Physiology* **104,** 339–347.

Clough SJ, Bent AF. 1998. Floral dip, a simplified method for *Agrobacterium*-mediated transformation of *Arabidopsis thaliana*. *The Plant Journal* **16,** 735–743.

Deng XW, Caspar T, Quail PH. 1991. *cop1*, a regulatory locus involved in light-controlled development and gene expression in *Arabidopsis*. *Genes & Development* **5,** 1172–1182.

Debeaujon I, Peeters AJM, Leon-Kloosterziel KM, Koorneef M. 2001. The *TRANSPARENT TESTA12* gene of *Arabidopsis* encodes a multidrug secondary transporter-like protein required for flavonoid sequestration in vacuoles of the seed coat endothelium. *The Plant Cell* **13,** 853–871.

Diener AC, Gaxiola RA, Fink GR. 2001. *Arabidopsis ALF5*, a multidrug efflux transporter gene family member, confers resistance to toxins. *The Plant Cell* **13,** 1625–1637.

Ding Z, Wang B, Moreno I, *et al*. 2012. ER-localized auxin transporter PIN8 regulates auxin homeostasis and male gametophyte development in *Arabidopsis*. *Nature Communications* **3,** 941.

Fagard M, Desnos T, Desprez T, Goubet F, Refregier G, Mouille G, McCann M, Rayon C, Vernhettes S, Hofet H. 2000. *PROCUSTE1* encodes a cellulose synthase required for normal cell elongation specifically in roots and dark-grown hypocotyls of *Arabidopsis. The Plant Cell* **12,** 2409–2423.

Fan JL, Quan S, Orth T, Awai C, Chory J, Hu JP. 2005. The *Arabidopsis* PEX12 gene is required for peroxisome biogenesis and is essential for development. *Plant Physiology* **139,** 231–239.

Feng S, Martinez C, Gusmaroli G, *et al*. 2008. Coordinated regulation of *Arabidopsis thaliana* development by light and gibberellins. *Nature* **451,** 475–479.

Foresti O, daSilva LL, Denecke J. 2006. Overexpression of the *Arabidopsis* syntaxin PEP12/SYP21 inhibits transport from the prevacuolar compartment to the lytic vacuole in vivo. *The Plant Cell* **18,** 2275–2293.

Geldner N, Dénervaud-Tendon V, Hyman DL, Mayer U, Stierhof YD, Chory J. 2009. Rapid, combinatorial analysis of membrane compartments in intact plants with a multicolor marker set. *The Plant Journal* **59,** 169–178.

Geldner N, Hyman DL, Wang X, Schumacher K, Chory J. 2007. Endosomal signaling of plant steroid receptor kinase BRI1. *Genes & Development* **21,** 1598–1602.

Gendre D, Oh J, Boutté Y, *et al*. 2011. Conserved *Arabidopsis* ECHIDNA protein mediates trans-Golgi-network trafficking and cell elongation. *Proceedings of the National Academy of Sciences, USA* **108,** 8048–8053.

Halliday KJ, Martinez-Garcia JF, Josse EM. 2009. Integration of light and auxin signaling. *Cold Spring Harbor Perspectives in Biology* **1,** a001586.

Jiao Y, Lau OS, Deng XW. 2007. Light-regulated transcriptional networks in higher plants. *Nature Reviews Genetics* **8,** 217–230.

Jefferson RA. 1987. Assaying chimeric genes in plants, the GUS gene fusion system. *Plant Molecular Biology Reporter* **5,** 387–405.

Lau OS, Deng XW. 2010. Plant hormone signaling lightens up, integrators of light and hormones. *Current Opinion in Plant Biology* **13,** 571–577.

Leyser O, Day S. 2009. Light. In: *Mechanisms in Plant Development* . Blackwell Publishing, 138–161.

Li J, Nagpal P, Vitart V, McMorris TC, Chory J. 1996. A role for brassinosteroids in light-dependent development of *Arabidopsis*. *Science* **272,** 398–401.

Li L, He Z, Pandey GK, Tsuchiya T, Luan S. 2002. Functional cloning and characterization of a plant efflux carrier for multidrug and heavy metal detoxification. *The Journal of Biological Chemistry* **277,** 5360–5368.

Li R, Li J, Li S, *et al*. 2014. ADP1 affects plant architecture by regulating local auxin biosynthesis. *PLoS Genetics* **10,** e1003954.

Magalhaes JV, Liu J, Guimarães CT, *et al*. 2007. A gene in the multidrug and toxic compound extrusion (MATE) family confers aluminum tolerance in sorghum. *Nature Genetics* **39,** 1156–1161.

Marinova K, Pourcel L, Weder B, Schwarz M, Barron D, Routaboul JM, Debeaujon I, Klein M. 2007. The *Arabidopsis* MATE transporter TT12 acts as a vacuolar flavonoid/H^+ -antiporter active in proanthocyanidin-accumulating cells of the seed coat. *The Plant Cell* **19,** 2023–2038.

Miséra S, Muller AJ, Weiland-Heidecker U, Jürgens G. 1994. The *FUSCA* genes of *Arabidopsis*, negative regulators of light responses. *Molecular and General Genetics MGG* **244,** 242–252.

Monk BC, Goffeau A. 2008. Outwitting multidrug resistance to antifungals. *Science* **321,** 367–369.

Morita Y, Kataoka A, Shiota S, Mizushima T, Tsuchiya T. 2000. NorM of *Vibrio parahaemolyticus* is a Na^+-driven multidrug efflux pump. *Journal of Bacteriology* **182,** 6694–6697.

Morita Y, Kodama K, Shiota S, Mine T, Kataoka A, Mizushima T, Tsuchiya T. 1998. NorM, a putative multidrug efflux protein, of *Vibrio parahaemolyticus* and its homolog in *Escherichia coli*. *Antimicrobial Agents and Chemotherapy* **42,** 1778–1782.

Nawrath C, Heck S, Parinthawong N, Metraux J-P. 2002. EDS5, an essential component of SA-dependent signaling for disease resistance in *Arabidopsis*, is a member of the MATE-transporter family. *The Plant Cell* **14,** 275–286.

Nelson BK, Cai X, Nebenführ A. 2007. A multicolored set of in vivo organelle markers for co-localization studies in *Arabidopsis* and other plants. *The Plant Journal* **51,** 1126–1136.

Nikaido H. 2009. Multidrug resistance in bacteria. *Annual Review of Biochemistry* **78,** 119–146.

Noh B, Bandyopadhyay A, Peer WA, Spalding EP, Murphy AS. 2003. Enhanced gravi- and phototropism in plant *mdr* mutants mislocalizing the auxin efflux protein PIN1. *Nature* **424,** 999–1002.

Downloaded from https://academic.oup.com/jxb/article/66/20/6327/552696 by guest on 24 April 2024

Noh B, Murphy AS, Spalding EP. 2001. *Multidrug Resistance*-like genes of *Arabidopsis* required for auxin transport and auxin-mediated development. *The Plant Cell* **13,** 2441–2454.

Oh E, Zhu JY, Wang ZY. 2012. Interaction between BZR1 and PIF4 integrates brassinosteroid and environmental responses. *Nature Cell Biology* **14,** 802–809.

Pelletier S, Van Orden J, Wolf S, *et al*. 2010. A role for pectin de-methylesterification in a developmentally regulated growth acceleration in dark-grown *Arabidopsis* hypocotyls. *New Phytologist* **188,** 726–739.

Reed JW, Nagpal P, Poole DS, Furuya M, Chory J. 1993. Mutations in the gene for the red/far-red light receptor phytochrome B alter cell elongation and Physiologyogical responses throughout *Arabidopsis* development. *The Plant Cell* **5,** 147–157.

Rogers EE, Guerinot ML. 2002. FRD3, a member of the multidrug and toxin efflux family, controls iron deficiency responses in *Arabidopsis*. *The Plant Cell* **14,** 1787–1799.

Seo PJ, Park J, Park M-J, Kim S-G, Jung J-H, Park C-M. 2012. A golgi-localized MATE transporter mediates iron homoeostasis under osmotic stress in *Arabidopsis*. *Biochemical Journal* **442,** 551–561.

Serrano M, Wang B, Aryal B, Garcion C, Abou-Mansour E, Heck S, Geisler M, Mauch F, Nawrath C, Metraux JP. 2013. Export of salicylic acid from the chloroplast requires the multidrug and toxin extrusion-like transporter EDS5. *Plant Physiology* **162,** 1815–1821.

Shao J, Liu X, Wang R, Zhang G, Yu F. 2012. The over-expression of an *Arabidopsis* B3 transcription factor, ABS2/NGAL1, leads to the loss of flower petals. *PLoS One* **7,** e49861.

Spitzer C, Reyes FC, Buono R, Sliwinski MK, Haas TJ, Otegui MS. 2009. The ESCRT-related CHMP1A and B proteins mediate multivesicular body sorting of auxin carriers in *Arabidopsis* and are required for plant development. *The Plant Cell* **21,** 749–766.

Sun X, Gilroy EM, Chini A, Nurmberg PL, Hein I, Lacomme C, Birch PRJ, Hussain A, Yun B-W, Loake GJ. 2011. *ADS1* encodes a MATE-transporter that negatively regulates plant disease resistance. *New Phytologist* **192,** 471–482.

Viotti C, Bubeck J, Stierhof YD, *et al*. 2010. Endocytic and secretory traffic in *Arabidopsis* merge in the trans-Golgi network/early endosome, an independent and highly dynamic organelle. *The Plant Cell* **22,** 1344–1357.

Wang M, Liu X, Wang R, Li W, Rodermel S, Yu F. 2012. Overexpression of a putative *Arabidopsis* BAHD acyltransferase causes dwarfism that can be rescued by brassinosteroid. *Journal of Experimental Botany* **63,** 5787–5801.

Xiang C, Han P, Lutziger I, Wang K, Oliver DJ. 1999. A mini binary vector series for plant transformation. *Plant Molecular Biology* **40,** 711–717.

Yoo SD, Cho YH, Sheen J. 2007. *Arabidopsis* mesophyll protoplasts, a versatile cell system for transient gene expression analysis. *Nature Protocols* **2,** 1565–1572.

Yu F, Liu X, Alsheikh M, Park S, Rodermel S. 2008. Mutations in SUPPRESSOR OF VARIEGATION1, a factor required for normal chloroplast translation, suppress *var2*-mediated leaf variegation in *Arabidopsis*. *The Plant Cell* **20,** 1786–1804.

Yu F, Park S, Rodermel SR. 2004. The *Arabidopsis* FtsH metalloprotease gene family, interchangeability of subunits in chloroplast oligomeric complexes. *The Plant Journal* **37,** 864–876.

Zhao J, Dixon RA. 2009. MATE transporters facilitate vacuolar uptake of epicatechin 3′-O-glucoside for proanthocyanidin biosynthesis in *Medicago truncatula* and *Arabidopsis*. *The Plant Cell* **21,** 2323–2340.

Zhao Y, Christensen SK, Fankhauser C, Cashman JR, Cohe JD, Weigel D, Chory J. 2001. A role for flavin monooxygenase-like enzymes in auxin biosynthesis. *Science* **291,** 306–309.

Downloaded from https://academic.oup.com/jxb/article/66/20/6327/552696 by guest on 24 April 2024